KSCE Journal of Civil Engineering (2024) 28(8):3270-3285
DOI 10.1007/s12205-024-1161-x

pISSN 1226-7988, eISSN 1976-3808
www.springer.com/12205

Hydraulic Engineering

Local Scour Depth Around Bridge Piers: Performance Evaluation of Dimensional Analysis-based Empirical Equations and AI Techniques

Abdul Razzaq Ghumman[a], **Husnain Haider**[a], **Ibrahim Saleh Al Salamah**[a], **Md. Shafiquzzaman**[a], **Abdullah Alodah**[a], **Mohammad Alresheedi**[a], **Rashid Farooq**[b], **Afzal Ahmed**[c], and **Ghufran Ahmed Pasha**[c]

[a]*Dept. of Civil Engineering, College of Engineering, Qassim University, Buraydah 51452, Saudi Arabia*
[b]*Dept. of Civil Engineering, International Islamic University, Islamabad 44000, Pakistan*
[c]*Dept. of Civil Engineering, University of Engineering and Technology, Taxila 47050, Pakistan*

ARTICLE HISTORY

Received June 12 2023
Revised December 2 2023
Accepted March 25 2024
Published Online 31 May 2024

KEYWORDS

Bridge pier
Scour depth
Artificial intelligence
Artificial neural network
Reduced gradient

ABSTRACT

Artificial Intelligence (AI) techniques, such as Artificial Neural Networks (ANN) and Adaptive Neuro-Fuzzy Inference Systems (ANFIS), and dimensional analysis-based empirical equations (DAEEs), can estimate scour depth around bridge piers. AI's accuracy depends on various architectures, while DAEEs' performance depends on experimental data. This study evaluated the performance of AI and DAEEs for scour depth estimation using flow velocity, depth, size of bed sediment, critical approach velocity, and pier width. The data from a smooth rectangular (20 m × 1 m) flume and a high-precision particle image velocimetry to study the flow structure around the pier - width: 1.5 – 91.5 cm evaluated DAEEs. Various ANNs (5, 10, and 15 neurons), double layer (DL) and triple layers (TL), and different ANFIS settings were trained, tested, and verified. The Generalized Reduced Gradient optimization identified the parameters of DAEEs, and Nash–Sutcliffe efficiency (NSE) and Mean Square Error (MSE) evaluated the performance of different models. The study revealed that DL ANN-3 with 10 neurons (NSE = 0.986) outperformed ANFIS, other ANN (ANN1, ANN2, ANN4 & ANN5) models, and empirical equations with NSE values between 0.76 and 0.983. The study found pier dimensions to be the most influential parameter for pier scour.

1. Introduction

Bridges are expensive hydraulic structures vital in facilitating transportation systems and boosting the national economy. Some bridges, especially over wadies in arid regions like Saudi Arabia, have long spans, and failure of such hydraulic structures can cause devastating socio-economic losses (Youssef et al., 2021; Alharbi and Mills, 2022). Natural disasters like floods and earthquakes may damage the foundation of bridges. Many studies worldwide have identified scour as one of the most critical aspects in the failure of bridge foundations (Huang et al., 2016; Ciancimino et al., 2022; Farooq et al., 2021; Zhang et al., 2022). Instead of super or sub-structure, scouring around the piers and abutments leads to the failure of bridges every year around the world (Fouli and Elsebaie, 2016; Huang et al., 2016). Building a bridge across a waterway with its foundation consisting of columns and piers alters the natural flow conditions. The piers reduce the flow path, which changes the flow pattern due to the development of eddies, turbulences, undercutting currents, and vortices. All these changes eventually result in scouring, essentially removing bed and channel banks' material by water, particularly from the areas near the bridge piers and abutments. A scour pit is produced by this phenomenon, reducing the depth of the foundation, thereby reducing the foundation's bearing capacity underneath strata (Hassan et al., 2022; Pregnolato et al., 2022; Zhang et al., 2022).

As stated above, it is a highly complex phenomenon resulting from an interaction between the bed material and turbulent flow. In some cases, downward seepage affects the scour depth around the bridge pier and needs to be considered in scour depth investigations. In the case of downward seepage, Reynolds stress, higher order moments, and sediment transport significantly impact scouring around bridge piers and must be appropriately analyzed.

CORRESPONDENCE Husnain Haider h.chaudhry@qu.edu.sa Dept. of Civil Engineering, College of Engineering, Qassim University, Buraydah 51452, Saudi Arabia

Another point worth considering when scouring around bridge piers is when the structure faces a current of water flow. The flow in such conditions accelerates around the bridge pier, so the vertical velocity gradient is converted to a pressure gradient acting on the pier surface. The pressurized flow causes a downward current and impacts the bed, increasing scour depth significantly. These critical aspects of scouring around bridge piers have been studied in past research, and results can be seen from published literature (Chavan et al., 2019; Chavan and Kumar, 2020).

Imhof (2004) gathered comprehensive bridge failure data worldwide and found that usual hazards cause collapsing bridges, extending to nearly 30% of encountered cases (Hafez, 2016). Among the natural risks, scour, and floods are responsible for about 60% of the cases of bridge failure worldwide (Wardhana and Hadipriono, 2003; Maddison, 2012). The Federal Highway Administration (FHWA) investigated bridge failures in the USA and reported that 60% of such failures are mainly because of scour (Federal Highway Administration, 1988; Parola et al., 1997), nearly 55 to 60 bridges collapsing yearly. Between 1989 and 2000 in the USA, 500 bridges collapsed primarily because of floods and scour (Wardhana and Hadipriono, 2003). Lin et al. (2014) analyzed thirty-six historical cases of bridge collapse due to scour and found that around 40% of scour depths ranged between 0.5 and 5 m. They further reported a maximum scour depth of up to 15 m. About 64% of bridge collapse cases accounted for local scour, according to Lin et al. (2014). According to Annad et al. (2021) and Briaud et al. (1999), for a set of 600,000 bridges in the USA, out of 1,000 collapses, 50% were scour-related failures.

Realizing the importance of scour, the first step towards the safety of bridges and users against local scouring is correctly estimating the scour depth around bridge piers. The excessive scouring can lead to high maintenance costs or even a bridge collapse, which results in various socio-economic losses, such as expensive repairs, disruption of traffic, and possibly death of passengers traveling on the bridge at the time of failure (Farooq et al., 2021; Hassan and Jalal, 2021). Past studies reported many experimental, empirical, and computational techniques (equations based on laws of physics and Artificial Intelligence (AI) techniques) for the estimation of local scour depth (Pizarro et al., 2020; Annad et al., 2021; Farooq et al., 2021; Hassan and Jalal, 2021).

Recently, several studies assessed the efficiency of empirical equations to estimate local scour (Park et al., 2017; Wang et al., 2017; Namaee et al., 2018; Liang et al., 2019; Sharafati et al., 2020; Hamidifar et al., 2021). Mohammadpour (2017) developed empirical equations for predicting temporal variation in local scour and validated the equations by conducting experiments using clear water. Pizarro et al. (2017) developed a local scour estimation formula based on energy concepts and entropy theory. Omara et al. (2020) developed several equations to estimate local scour around bridge piers for shallow flow environments. They included the effects of the flow intensity, the angle of inclination of the circular pier with flow attack, and the length of the pier. Some recent studies applied Flow-3D numerical models to predict the local scour depth around hydraulic bridge piers (Fattah et al., 2018; Jalal and Hassan, 2020; Hassan and Jalal, 2021). Modern soft computations and data-dependent gene-expression programming based on laws of physics developed distributed Flow-3D. In most prevailed cases of scarce data, the assumptions adopted to solve the complicated equations may increase uncertainties in results.

Several studies developed data-driven formulae to predict the local scour depth using field observations and experimental data (Azamathulla et al., 2010; Khassaf and Ahmed, 2021; Hassan and Jalal, 2021). Such approaches applying dimensional analysis followed by numerical techniques lack precision, and results are liable to ambiguities (Cao et al., 2021). Scour depth depends on the soil type, and the clear-water flow phenomenon differs from live-bed scour (Arneson et al., 2012; Mohammadpour, 2017; Annad et al., 2021; Mohammadpour et al., 2021). The equations for estimating the local scour depth around bridge piers involve parameters including bridge pier shape and dimensions, sediment size, flow velocity, flow depth, and others that must be optimized (Akhlaghi et al., 2020; Dimitriadis et al., 2021; Saad et al., 2021). Hence, a generalized equation for all types of soils under different flow conditions can lead to erroneous outcomes (Hassan and Jalal, 2021). There is a difference of opinion and ambiguity in predicting scour depth and relating it to the field conditions. Consequently, most hydraulic bridge collapses arise from failures in oversight of the scour problem (Hassan and Jalal, 2021; Hassan et al., 2022; Pregnolato et al., 2022; Zhang et al., 2022). Some studies used optimized techniques to develop empirical formulae for scour depth estimation and compared the results with conventional equations (Afzali, 2016; Pandey et al., 2020; Annad et al., 2021). Although the studies claimed improved performance of newly developed equations, further research on optimizing parameters is warranted.

In addition to empirical equations, Artificial Intelligence (AI) techniques are becoming popular for estimating scour depth (Pal et al., 2011; Moussa, 2013; Onen, 2014; Dang et al., 2021; Hassan et al., 2022). Hassan et al. (2022) used three techniques for such analysis, including ANN, non-linear regression, and gene expression programming, and found ANN to be the best performer. Sarshari and Mullhaupt (2015) reported that Artificial Neural Network (ANN) models outperform empirical equations in estimating local scour depth. Oğuz and Bor (2021) also said the superiority of AI techniques over empirical equations. Hence, rapidly emerging AI techniques can predict the bridge scour depth with less effort and high accuracy (Muzzammil et al., 2015; Hassan et al., 2022). Nevertheless, past studies highlight several aspects of AI techniques demanding further investigations, such as the architecture of ANN and the choice of the best training function for ANN. The present study has taken up these aspects in depth to contribute to the knowledge about AI applications for scour depth prediction.

The topic of scour depth estimation needs further attention. Most of the past studies used laboratory data and dimensional analysis to investigate the scouring phenomenon around piers of

bridges (Sreedhara et al., 2021). The scouring phenomenon holds several intrinsic complexities due to natural flows in wadies and rivers. Bridge failures in the presence of several local scour formulas question the reliability of these equations and urge investigators for further research in two main dimensions. First, investigate the most significant parameters of empirical equations for accurate scour depth estimation. Second, evaluation of available methods to choose the best-performing method for predicting the local scour around the bridge piers. The present research addressed both aspects with the primary objectives to i) obtain data of the parameters required for sour depth estimation from available resources and additional data through experimental study, ii) identify significant parameters of local scour estimation in empirical equations using efficient optimization techniques, and iii) estimate local scour using various artificial intelligence (AI) methods.

2. Material and Methods

2.1 Study Framework

Figure 1 presents the overall methodological framework of the present study. The scour depth data was collected through experiments performed on a flume in a hydraulic laboratory and past studies to investigate various models and develop empirical equations. The study tested five types of Artificial Neural Networks (ANN) models and two Adaptive Neuro-Fuzzy Inference Systems (ANFIS) to select the models with high-performing architecture and training functions. Furthermore, the evaluation process considered double and triple layers of the five ANN models with three scenarios of the number of neutrons (5, 10, and 15) generating 30 scenarios. Nash–Sutcliffe efficiency (NSE) and Mean Square Error (MSE) evaluated the performance of ANN and ANFIS models. Analysis of variance (ANOVA) assessed the significance of training functions, number of neurons, and layers for ANN models. The evaluation process compared the results of the best-performing model from ANN and ANFIS with nine Dimensional Analysis-based Empirical Equations (DAEEs). Generalized Reduced Gradient (GRG) optimized the parameters of DAEEs. Finally, sensitivity analysis identified the most significant factors contributing to scour depth estimated by different techniques.

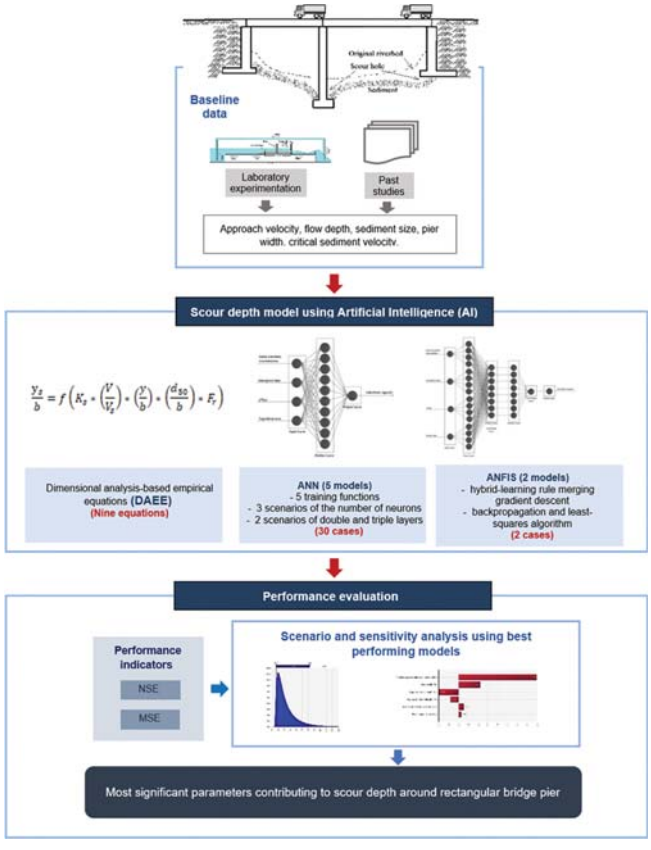

Fig. 1. Methodology for Scour Depth Prediction Modeling Around Bridge Piers Using AI and DAEE

2.2 Baseline Data Collection

Figure 2 illustrates the experimental setup used in the present study. The present study investigated scour depth by a rectangular hydraulic flume consisting of 12 mm thick glass walls and a concrete base. The flume contained an inlet, a working section in the middle of the flume, and an outlet. The main channel of the flume was 20 m long, 1 m wide, and 0.75 m high. An inflow pipe transferred water from the source to the flume inlet. Water passes through a water circulation arrangement at the inlet of the flume to obtain smooth and fully developed flow conditions.

The flume bed (0.3 m width × 6 m length) contained fine and uniformly graded sand. A wooden pier was fixed in the middle of the sand bed. Small stones were used at the front side of the sand bed to obtain a steady transition between the concrete and the sand bed. A mobile point gauge monitored the bed levels and water surface levels. The particle image velocimetry (PIV) observed the flow structure around the bridge pier. A rectangular weir was installed at the channel's end for discharge measurement. Similar flow conditions were maintained for all experiments. The Vernier point gauge observed the bed profile, which can move in all three directions (transverse, longitudinal, and vertical), with a 0.05 mm least count. A small silting basin at the end of the channel avoided the mixing of sediments with water, as the sediments can get eroded during the experimental runs, leading to scouring around the pier. An outflow pipe at the end of the silting basin kept the flow uniform. Table 1 describes the experimental data's minimum, mean, and maximum values. In addition to laboratory experiments, other data was collected from various publications (Benedict and Caldwell, 2014; Chabert, 1956; Ettema, 1980; Melville, 1984).

2.3 Dimensional Analysis-Based Empirical Equations

The local scour-depth y_s around a bridge-pier in clear water, steady-state flow over a bed of uniform material, and non-cohesive sediments condition depend on several variables, including the velocity of water (V), the depth of flow (y), the median size of bed sediment (d_{50}), critical approach velocity (V_c), pier width/diameter (d), the shape factor of the pier (K_s), and flow duration (t) (also see Table 1). Therefore, the scour depth (y_s) can be described

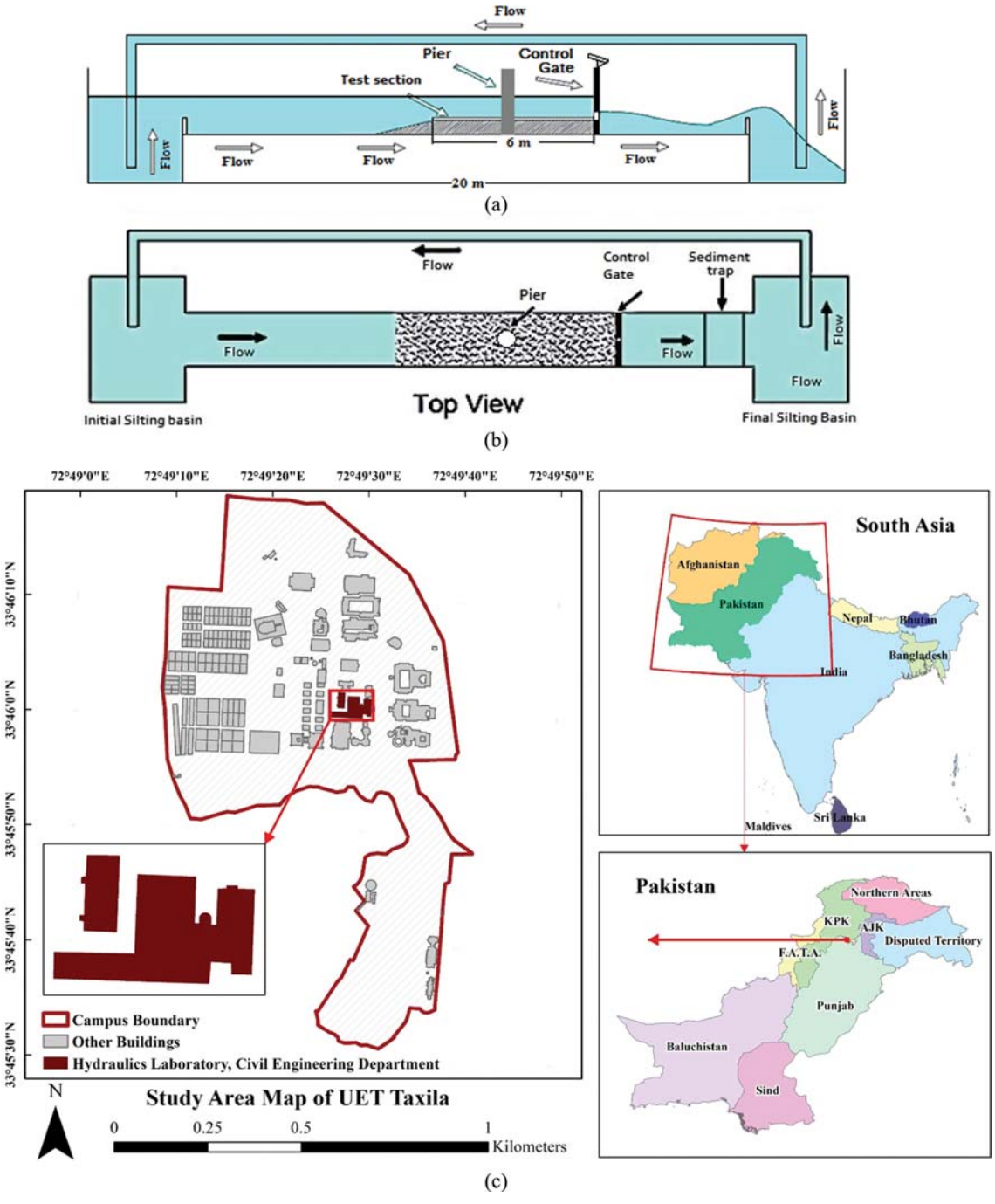

Fig. 2. Experimental Rectangular Flume, (a) Cross-Section, (b) Top View, (c) Site Map

Table 1. Minimum, Mean, and Maximum Values of Experimental Data

Experimental range	Pier width "b" (cm)	Approach flow velocity "V" (cm/s)	Sediment Critical Velocity "V_c" (cm/s)	Approach Flow Depth "y" (cm)	Median size of bed sediments "d_{50}" (mm)
Minimum	1.5	14.9	22.0	2.0	0.2
Mean	6.0	0.37	40.0	14.0	0.96
Maximum	91.5	215.8	127.5	190	7.8

as a function of all these variables, presented as $y_s = f(V, y, d_{50}, V_c, b, K_s, t)$, and the dimensional analysis was applied to these dimensional variables using the Buckingham's π-theorem as:

$$\frac{y_s}{b} = f\left(K_s * \left(\frac{V}{V_s}\right) * \left(\frac{d_{50}}{b}\right) * F_r\right). \quad (1)$$

The study tested the following DAEEs:

$$y_s = k_s * (b)^{C_1} * (Fr)^{C_2}, \quad (2)$$

$$y_s = k_s * \left(\frac{y}{b}\right)^{C_1} * (Fr)^{C_2}, \quad (3)$$

$$y_s = k_s * \left(\frac{b}{y}\right)^{C_1} * (Fr)^{C_2}, \quad (4)$$

$$y_s = k_s * \left(\frac{b}{y}\right)^{C_1} * y * (Fr)^{C_2}, \quad (5)$$

$$y_s = k_s * \left(\frac{b}{b}\right)^{C_1} * b * (Fr)^{C_2}, \quad (6)$$

$$y_s = k_s * \left(\frac{y}{b}\right)^{C_1} * b, \quad (7)$$

$$y_s = k_s * \left(\frac{b}{y}\right)^{C_1} * y, \quad (8)$$

$$y_s = k_s * \left(\frac{b}{y}\right)^{C_1} * d_{50} * \left(\frac{V}{V_c}\right)^{C_2}, \quad (9)$$

$$y_s = k_s * \left(\frac{b}{y}\right)^{C_1} * d_{50} * \left(\frac{v_c}{V}\right)^{C_2}, \quad (10)$$

where Fr is the Froude Number and C_1 and C_2 are empirical constants.

2.4 Artificial Neural Networks

Many studies have adopted ANN due to its applicability to various hydrological modeling problems. An ANN model consists of input, hidden, and output layers. The neurons, the fundamental determining entities of an ANN model, perform calculations using many inputs and compare the output with a target value. An internal structural procedure performs training, validation, and testing processes. The data is generally divided into three parts: training, validation, and testing. Although the common practice is to use 60% for training, 20% for validation, and 20% for testing, other ratios, such as 70%, 15%, and 15%, and 50%, 25%, 25% have also been used in practice. There are two types of data division: 70%, 15%, and 15%. The first approach randomly selects the ratio 70%, 15%, and 15%. In comparison, the second approach first uses 70% of the data for training, selects the first half of the remaining data (20% of the whole data set) for validation, and uses the last part for testing. We randomly selected 70%, 15%, and 15% for training, validation, and testing. The feed-forward mechanism of hidden layers works out the backpropagation (BP) for generating accurate outputs. If there are multiple hidden layers, it is termed a Multi-Layer Perceptron (MPL). Out of several training functions, the present study used five different types of training functions described in Table 2, which were accordingly named ANN-1, ANN-2, ANN-3, ANN-4, and ANN-5. The present study further divided the five ANN models into sub-categories conditioned by double and triple hidden layers, represented by double-layer (DL) and triple-layer (TL) models.

Furthermore, the number of neurons may vary in the hidden layers (Sheela and Deepa, 2013). Past studies have employed the hit-and-trial method to select neurons' numbers (Arifin et al., 2019; Ogunbo et al., 2020). The present study adopted the approach of choosing the same number of neurons in DL or TL. Accordingly, the present study tested the architectures of 5, 10, and 15 neurons for DL and TL. Fig. 3(a) illustrates the adopted ANN approach for estimating scour depth. There are two main types of learning concerning supervision. It can be supervised or unsupervised. Suppose the target is given, and error can be estimated by determining the difference between the simulated and measured values. In that case, it is called supervised learning, and if the measured data is not provided and ANN has to generate some logic to reach the final simulation results, then it is called unsupervised learning. In the present study, supervised learning was used.

Table 2. Various Training Functions of ANN

Model	Function	Description of the training function
ANN-1	Trainlm	Levenberg-Marquardt BP
ANN-2	Trainbr	Bayesian regularization
ANN-3	Trainbfg	BFGS Quasi-Newton BP
ANN-4	Trainrp	Resilient backpropagation (Rprop)
ANN-5	Trainscg	Scaled conjugate gradient BP

2.5 Adaptive Neuro-Fuzzy Inference Systems

Adaptive Neuro-Fuzzy Inference Systems (ANFIS) comprises an adaptive ANN and a fuzzy inference system. ANFIS applies a hybrid-learning rule merging gradient descent, backpropagation, and a least-squares algorithm for parameter prediction. Fig. 3(b) shows the 5-layered structure of ANFIS. Layer 1 is the fuzzy layer; every node in this layer is called an adaptive node. The present study adopted generalized bell and Gaussian membership functions. In Layer 2- the product layer, the firing strength of a rule is shown as the node's output. Layer 3- the normalized layer shows the rules' normalized firing strength. Layer 4- the de-fuzzy layer indicates the rules' contribution towards the complete output. Layer 5- the total output layer represents the defuzzified (single) valued output. In ANFIS, a "membership function" plays a crucial role in determining the accuracy of the outputs through a well-defined process of mapping inputs into the outputs. The membership function consists of a curve representing inputs, so a function was given a specific name based on the shape of the curve. Table 3 describes the two tested types of ANFIS models.

2.6 Performance Evaluation

Two performance indicators, NSE and MSE, were used to assess the degree of accuracy of predictions resulting from the methods mentioned above. Eq. (11) gives the formula for NSE (Moriasi et al., 2007).

$$NSE = \left(1 - \frac{\sum_{i=1}^{n}(ys_{mi} - ys_{pi})^2}{\sum_{i=1}^{n}(ys_{mi} - \overline{ys}_{mi})^2}\right) \quad (11)$$

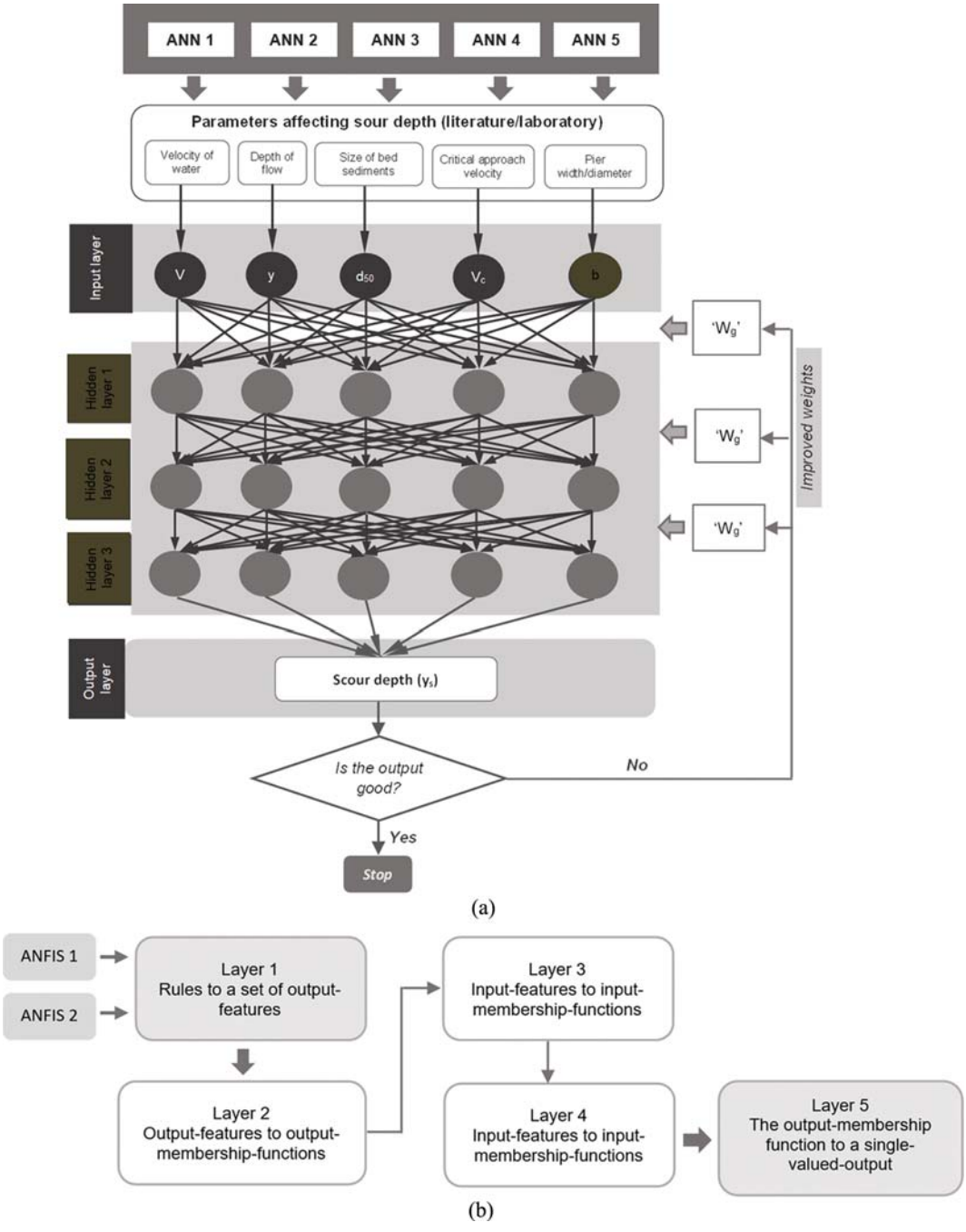

Fig. 3. AI Models Used in the Study, (a) Multi-Layer ANN, (b) 5-Layer ANFIS Structure

Table 3. Various Membership Functions of ANFIS

Model	Function	Description of Training Function
ANFIS-1	*Gbellmf*	"Gbellmf" is a bell-shaped membership function having three types of parameters to define the bell-shaped curve. The curve width is defined by one parameter, the other parameter is simply a positive integer, while the third parameter defines the curve-center
ANFIS-2	*Trapmf*	"Trapmf" is a Trapezoidal membership function having four types of parameters that define the curve. Two parameters define the feet and the other two are to define the shoulders of the curve as it has the shape of a truncated triangle

Table 4. Performance Levels for Evaluation of the Developed Models (Moriasi et al., 2007)

NSE range	Performance level
0.75 to 1.00	Very Good
0.65 to 0.75	Good
0.50 to 0.65	Satisfactory
0.4 to 0.50	Acceptable
≤ 0.4	Unsatisfactory

ys_{mi} presents recorded scour depth for the ith measured value, ys_{pi} denotes predicted scour depth for the same data point, $\overline{ys}_{mi}$ is mean scour depth, and n is the total data points used for models' testing. Table 3 presents the performance for model evaluation.

The MSE was estimated using the following equation:

$$MSE = \frac{\sum_{i=1}^{n}(ys_{mi} - ys_{pi})^2}{n}. \quad (12)$$

The present research does not include the epochs' numbers and the ANN computation time due to their insignificance in hydrological studies. Table 4 describes the performance levels for the evaluation of the developed models.

2.7 General Reduced Gradient Method of Optimization

The recent optimization techniques can solve non-linear problems in hydraulic phenomena. The main goal of such optimization techniques is the global maximization or minimization of the objective function by adjusting values of some parameters of an equation describing a hydraulic phenomenon, for instance, scour depth around a bridge in the present case. The objective function is usually one of the statistical parameters based on the difference between the observed and predicted data. The current research maximized NSE to '1' and minimized MSE to a given error limit.

Problems consisting of non-linear functions are more challenging to solve than linear ones. Several techniques are available to date for solving problems regarding the non-linear phenomenon. The general reduction gradient (GRG) technique is a readily available and efficient optimization method for solving non-linear hydraulic problems (Abadie, 1969; Lasdon et al., 1978). Fig. 4 illustrates the flowchart of the GRG process. Hence this technique has been adopted to identify the parameters of empirical equations for estimating local bridge pier scour depth.

$$\text{Maximize/Minimize } O(v),\ v \in F_s \subseteq W_s, \quad (13)$$

$$\text{Subject to } \begin{matrix} E_i(v) = 0, & i = 1, \ldots\ldots, p, \\ b_l \le v_k \le b_u & k = 1, \ldots\ldots, n, \end{matrix} \quad (14)$$

where v is a vector with n variables, $O(v)$ is the objective function, $E_i(v)$ (i = 1,..., p where $p < n$) denotes the i^{th} constraint, the symbol W_s represents the whole search space, F_s defines the feasible search space, and b_u and b_l represents the upper and lower bounds of the variable v_k(k = 1, ..., n). All the functions in the above equations are differentiable. The GRG method solves a system of un-constrained non-linear programs in a reduced dimension space, a manifold defined by the non-linear equations. The study checked the objective functions for every solution and stopped after approaching a constrained global optimal solution (Fig. 4).

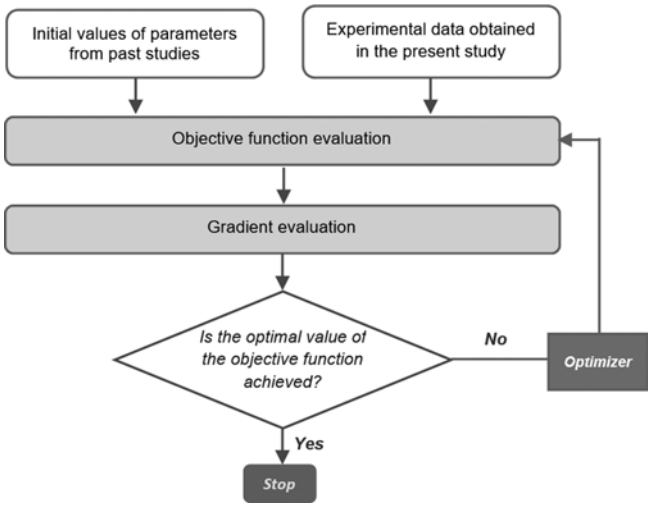

Fig. 4. Flowchart for Reduced Gradient Optimization for Identification of Parameters of DAEE

2.8 Input Combinations for ANN and Sensitivity Analysis of Parameters for DAEE

This section describes investigating the input combinations for ANN and ANFIS. As ANN models are data-driven, the training of such models depends on some input variables. These models pick up the relationship between the input variables and the output, even if this relationship is complex and cannot be expressed directly. So, choosing input parameters is an essential step in applying ANN models. The present research highlights the importance of various input variables by selecting different combinations. Sometimes, data regarding some variables is unavailable even if this particular variable has a strong relationship with the out variable. Hence, investigating the impact of the combination of input variables is valid even if the variables do not have any theoretical basis. However, the parameter selection should be based on the sensitivity analysis described at the end of this section and discussed in section 3.5.

Large data sets, 569 observations, were used through observed scour depths from past studies and laboratory experiments. Experiments performed at the University of Engineering and Technology Taxila, Pakistan, generated 60 data points. The number of input variables can significantly impact the simulation results, and many combinations may depend on the available data. The present study individually assessed each input's percentage effectiveness by using each input parameter (b, V, Vc, y, d_{50}) in the best-performing ANN and ANFIS models for each case by comparing the model output with the observed scour depth using NSE. The following five combinations (C1 – C5) of input variables were tested using ANN and ANFIS for the prediction of local

scour around a bridge pier:

1. C1 included the input variable b only
2. C2 included the input variables b and V
3. C3 included the input variables b, V, and Vc
4. C4 included the input variables b, V, Vc, y
5. C5 included the input variables b, V, Vc, y, d_{50}.

Sensitivity analyses identified the most critical factors contributing to the DAEE. Maximum, minimum, and average values were determined for the high-performing DA-based empirical equation. Subsequently, data for each parameter fitted to different probability distributions, such as Person-5, Inverse Gaussian, Gamma, and Lognormal, and the best-fitting probability distributions were adopted using licensed Version 8 of @Risk software. Finally, 5000 Montecarlo simulations identified the most significant parameter contributing to scour depth around the rectangular bridge pier.

3. Results and Discussion

3.1 Comparison of Various Architectures of ANN and Training Functions

Figure 5 shows the NSE and MSE values for training, validation, testing, and overall performance of all possible (30) combinations of ANN architectures and training functions. Scour depth was estimated using various architectures (5 neurons, 10 neurons, and 15 neurons with DL and TL) of ANN and training functions (ANN1 – ANN5) described in the above sections. Based on the overall performance, the DL ANN3 with 10 neurons shows the best performance, indicated by the highest overall NSE value of 0.986 with low MSE (0.0009).

Figure 6 illustrates the correlations between estimated and observed scour depth for five ANN models for various architectures and training functions, i.e., 5 DL and TL, 10 DL and TL, and 15

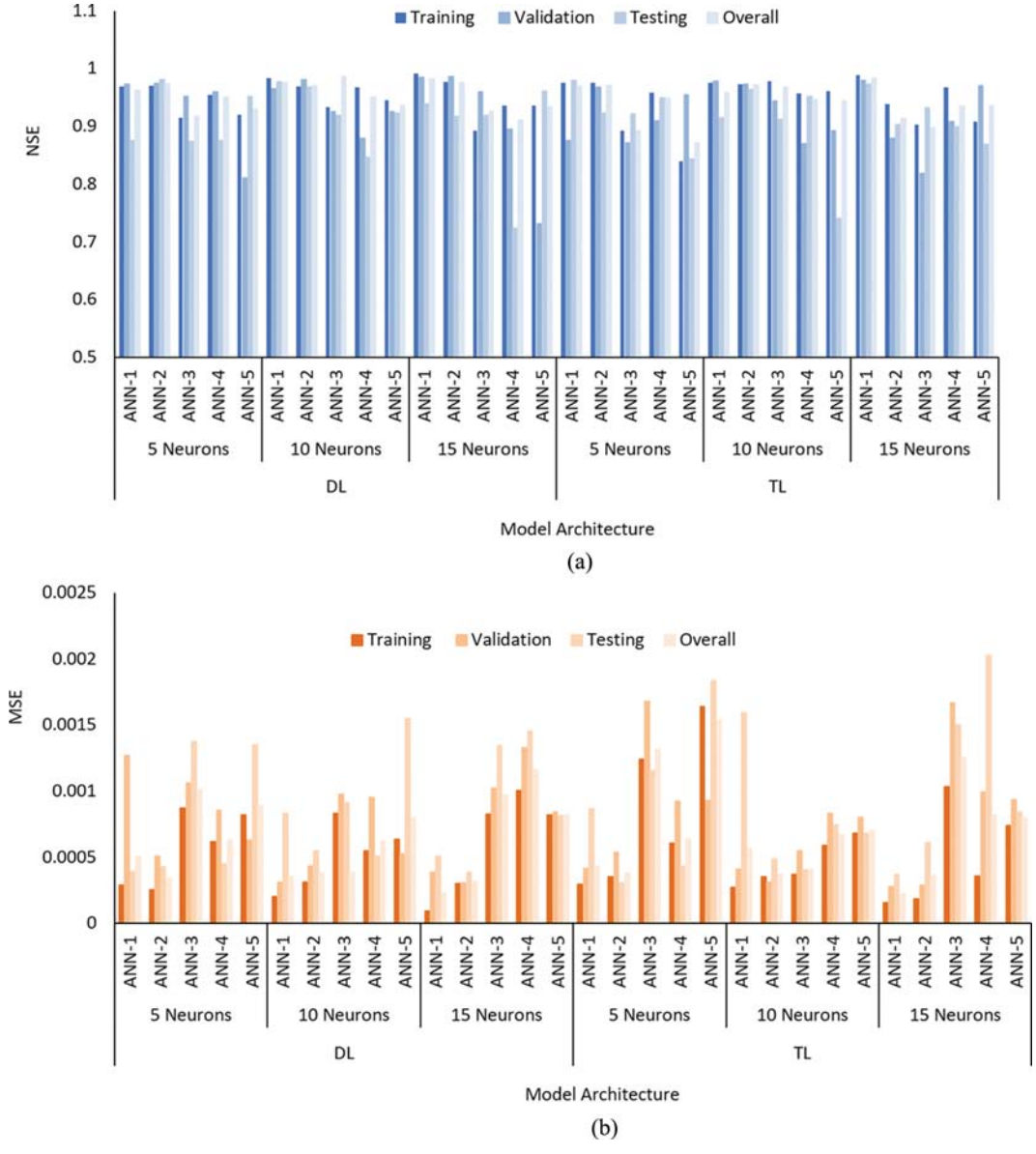

Fig. 5. ANN Modeling Results for Various Architectures and Training Functions, (a) MSE, (b) NSE

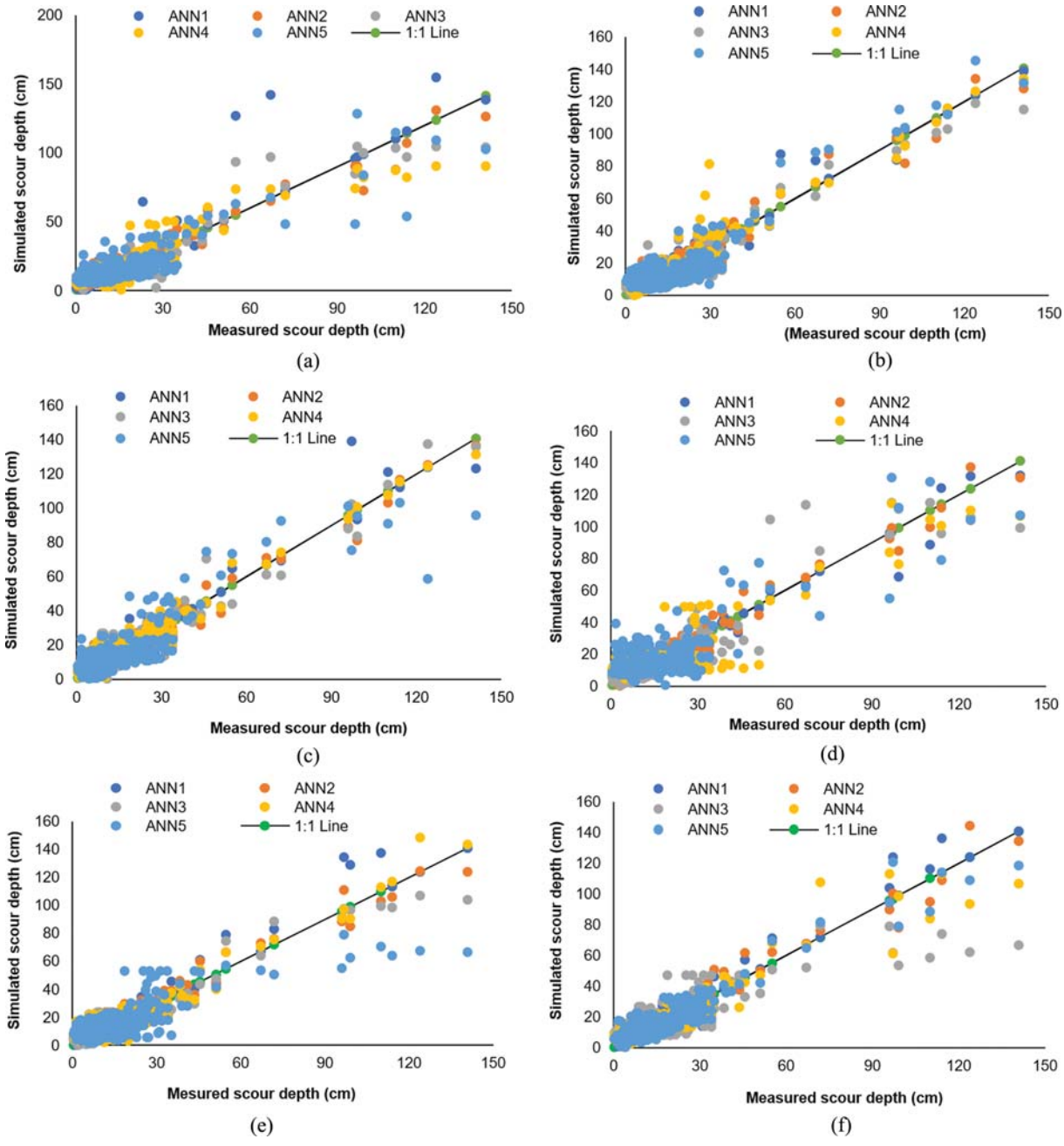

Fig. 6. Scour Depth Predicted by Five ANN Training Functions, (a) 5 Neurons (DL), (b) 10 Neurons (DL), (c) 15 Neurons (DL), (d) 5 Neurons-(TL), (e) 10 Neurons (TL), (f) 15 Neurons (TL)

DL and TL. All training functions performed well except ANN-2 (Bayesian Regularization training function) with 15 neurons in TL. Except ANN-2 with 15 neurons in TL, all other ANN models showed good performance with indices in "very good" range. The overall values of NSE ranged from 0.87 to 0.986, while MSE varied between 0.000153 and 0.000225. It is worth mentioning that NSE and MSE, in the case of ANN, are based on normalized values of observed and simulated local scour depth. The model ANN-3 outperformed the other models with an NSE value of 0.986 for DL with 10 neurons. The BFGS Quasi-Newton Backpropagation ANN-training function assessed scour depth around rectangular bridge piers. ANN-1 with 15 neurons obtaining an NSE value of 0.982 also showed comparable performance to ANN-3 with 10 neurons, which means the Levenberg-Marquardt Backpropagation training function can model scour depth with high accuracy.

In some cases, the values of NSE for training, validation, and testing are lower than the overall values of NSE. It is worth noting that the overall values of NSE are not the average value obtained for training, testing, and validation. Instead, it was calculated based on the simulated training, testing, and validation data. Eq. (11) shows that for smaller n values (the case of training,

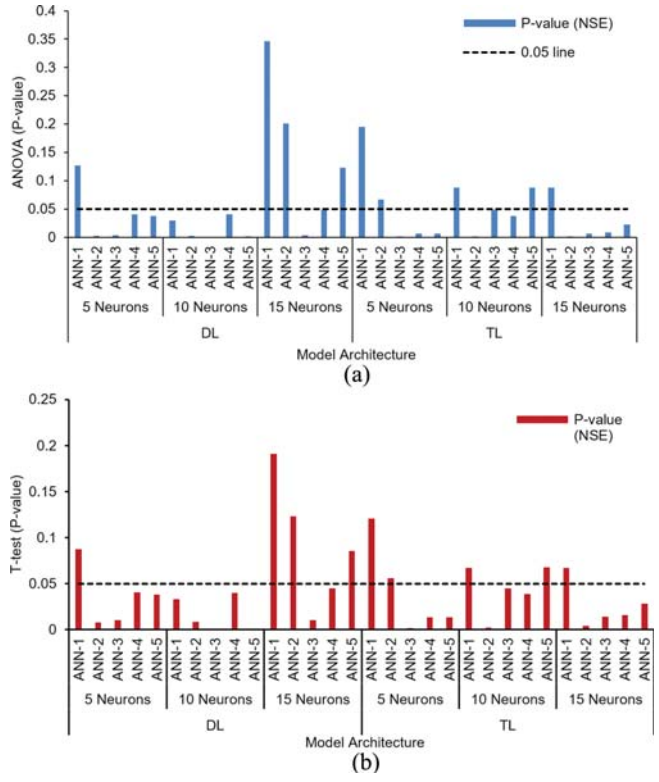

Fig. 7. Paired t-Test Results Comparing the NSE Value of the ANN-3 Model with 10 Neurons and a Double Layer (DL-10-ANN-3) Against All Other Models, (a) ANOVA, (b) T-Test

testing, and validation), the impact of any wrong simulated value will be higher, giving low values of NSE compared to values of NSE obtained for a higher number of data points or vice versa. The scatter plots in Figs. 6(a) – 6(f) also manifest that the Levenberg-Marquardt Backpropagation and the Quasi-Newton Backpropagation are close to the 1:1 line.

A one-way analysis of variance (ANOVA) assessed the differences in NSE values among the five ANN models (ANN-1, ANN-2, ANN-3, ANN-4, and ANN-5) and found both DL and TL ANN-3 models showed the least p-value and highest Fc for different neurons. Additionally, a paired t-test compared the NSE value of the ANN-3 model with 10 neurons and a double layer (DL-10-ANN-3) against all other models. The hypothesis is that there is a significant difference between the NSE value of DL-10-ANN-3 and all the other models ($p < 0.05$). Fig. 7 shows that most models show a p-value less than 0.05 against the ANOVA test (Fig. 7(a)) and T-test (Fig. 7(b)).

3.2 Comparison of ANFIS Models

Figure 8 shows highly likely results for the scour depth prediction around a bridge pier by two types of ANFIS models. Fig. 8(a) shows NSE values up to 0.98, whereas according to (Moriasi et al., 2007), the NSE values between 0.75 and 1 represent the top-level performance of a model. Choi and Choi (2022) reported high performance (NSE in the range of 0.75 to 0.9) in predicting scour depth by ANFIS in the training process. However, Abd El-Hady Rady (2020) found that genetic programming outperformed the ANFIS models. Section 2 explains that the ANFIS, consisting of a fuzzy inference system and an adaptive ANN model, combines backpropagation, gradient descent, and a least-squares algorithm for predicting local scour around a bridge pier. Fig. 8(b) illustrates that the hybrid approach of ANFIS produced highly accurate results for local scour depth around the bridge pier with a strong correlation between predicted and measured values.

3.3 Comparison of ANN-3 and ANFIS Models

Figure 9 compares the scour depth prediction results of ANN and ANFIS. The results show that the best ANN model (ANN3 with 10 neurons in the DL model) has a predicted scour depth around a bridge pier comparable to the ANFIS predicted scour depth. Although the ANFIS and ANN-3 showed high performance, the ANN3 models slightly outperformed the ANFIS models.

Figure 10 shows the results of scour depth predicted under various input combinations defined in section 2.6. The figure shows that the input combination C5&C4 produced the best scour depth results with an overall NSE value of 0.97 and an

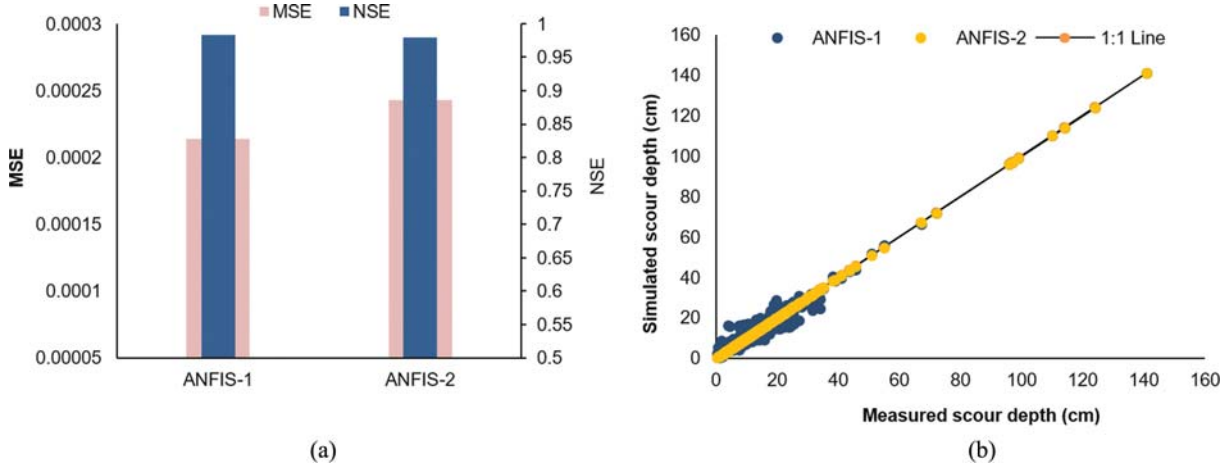

Fig. 8. Comparison of Predicted Scour Depth Around a Bridge Pier by 2 Types of ANFIS Models, (a) Performance Indices NSE & MSE, (b) Scatter Plot of the Simulated and Measured Scour Depth

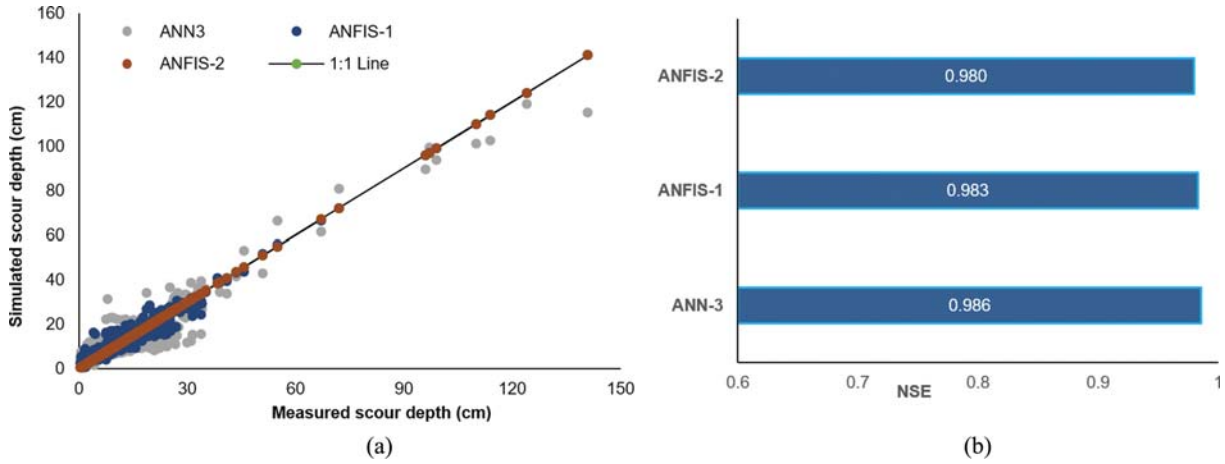

Fig. 9. Comparison of ANN-3 (DL with 10 neurons) with ANFIS-1 and ANFIS-2: (a) Correlation between Measured and Calculated Scour Depth, (b) NSE

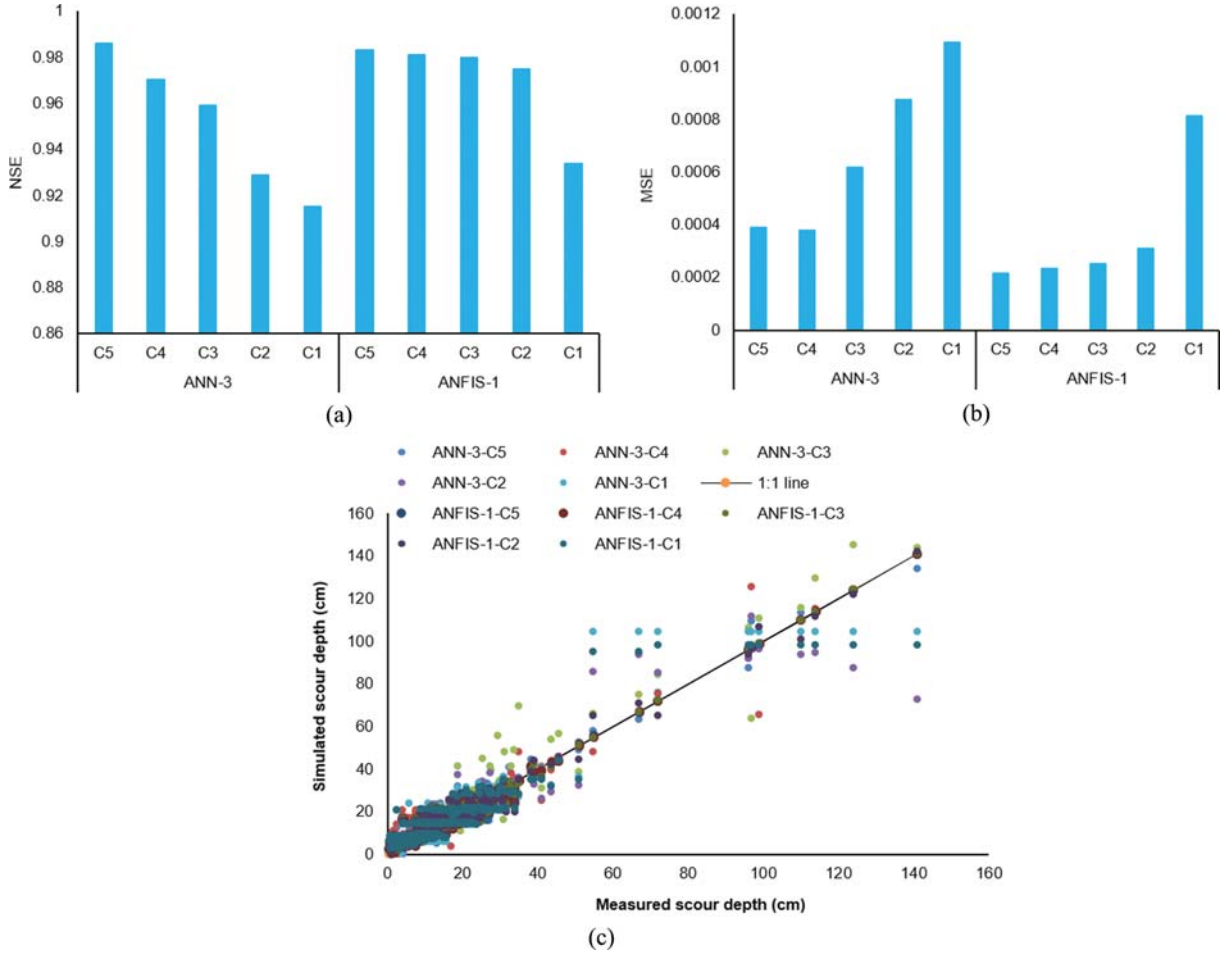

Fig. 10. Comparison of Scour Depth Predicted under Various Input Combinations: (a) NSE, (b) MSE, (c) Scatter Plot Showing Five Combinations for ANN-3 and ANFIS-1

MSE value of 0.00037. These findings indicate that the data-dependent AI-based techniques have higher accuracies when the number of input parameters is comparatively more significant. Nevertheless, the data collection for a higher number of input parameters is always challenging and costly.

3.4 Scour Depth Prediction Using Empirical Equations

Figure 11 shows the simulation results of scour depth around a bridge pier using nine DAEE. Figs. 9(a) – 9(c) shows that all the DAEE effectively simulated the scour depth around the bridge pier with acceptable accuracy. These simulations were performed by

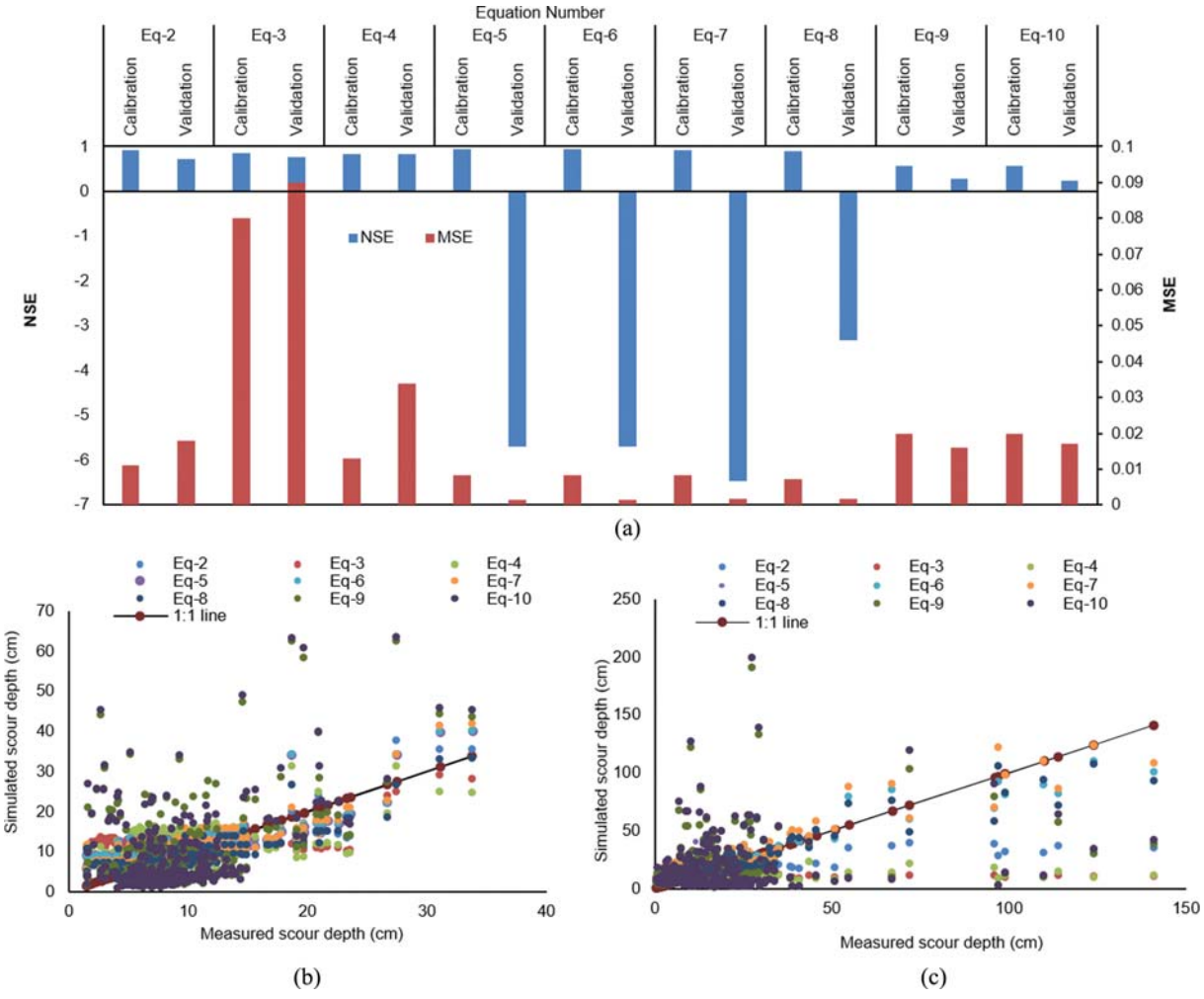

Fig. 11. Comparison of Results of Predicted Scour Depth from Various Empirical Equations, (a) NSE and MSE, (b) Calibration, (c) Validation

maximizing the NSE or minimizing the MSE as an objective function in reduced gradient optimization, as shown in Fig. 4. The results from minimizing MSE and maximizing NSE in the optimization process of parameters of nine DAEE are nearly similar in the two cases. Although Eqs. (2) – (7) are identical, some equations produced more accurate results. The values of NSE ranged from 0.76 to 0.93, with minimal values of MSE between 0.01 and 0.09. Table 5 compares the results of predicted scour depth from various empirical equations. Eqs. (5) and (6) outperformed (NSE = 0.931) the other DAEE in calibration, whereas Eqs. (3) and (4) performed better in calibration and validation (NSE values in the range of 0.76 to 0.86). Prediction of scour depth around the bridge piers using empirical equations is highly demanding. Annad and Lefkir (2022) and Cikojević et al. (2019) concluded that no universal DAEE could predict scour depth

3.5 Scenarios and Sensitivity Analysis

Scenario analyses identified the most important input parameters for scour depth prediction using best-performing ANFIS and ANN models. Monte Carlo-based sensitivity analysis performed a similar task for best performing DAEE, i.e., Eq. (10). Fig. 12(a) illustrates that AI-based models found pier width (b) as the most critical input variable, followed by the median size of bed sediments (d_{50}). At the same time, DAEE identified d_{50} as the most influential parameter, followed by pier width. Hence, these two inputs are the most critical parameters for scour depth prediction around bridge piers. Any change in these variables can highly impact scour depth around the bridge pier. Annad and Lefkir (2022) also assigned higher weights to b and d_{50} as they found these two parameters positively correlated with the scour depth.

4. Conclusions

ANN, ANFIS, and DAEEs investigated the local scour depth around a bridge pier. The study found that the performance of ANN3, with an NSE value of 0.986 and MSE of 0.0009, outranked ANFIS, other ANN models (ANN-1, ANN2, ANN4 & ANN5), and empirical equations with NSE values in the range of 0.76 to 0.983. ANN & ANFIS models perform better than empirical equations. No significant difference was observed between the two

Table 5. Comparison of Results of Predicted Scour Depth from Various Empirical Equations

NO	Equation	Optimized parameters			NSE		Performance NSE[1]		MSE	
		ks	C1	C2	Calibration	Validation	Calibration	Validation	Calibration	Validation
Eq-2	$y_s = k_s * (b)^{C_1} * (Fr)^{C_2}$	4.80	0.508	0.2	0.910	0.720	Very Good	Good	0.0110	0.0180
Eq-3	$y_s = k_s * \left(\frac{y}{b}\right)^{C_1} * (Fr)^{C_2}$	14.21	0.01	0.2	0.860	0.760	Very Good	Very Good	0.0800	0.0900
Eq-4	$y_s = k_s * \left(\frac{b}{y}\right)^{C_1} * (Fr)^{C_2}$	16.665	0.263	0.2	0.831	0.827	Very Good	Very Good	0.0130	0.0339
Eq-5	$y_s = k_s * \left(\frac{b}{y}\right)^{C_1} * y * (Fr)^{C_2}$	1.357	0.674	0.2	0.931	-5.691	Very Good	Not good correlation	0.0083	0.0014
Eq-6	$y_s = k_s * \left(\frac{y}{b}\right)^{C_1} * b * (Fr)^{C_2}$	1.357	0.326	0.2	0.931	-5.691	Very Good	Not good correlation	0.0083	0.0014
Eq-7	$y_s = k_s * \left(\frac{y}{b}\right)^{C_1} * b$	1.085	0.301	0.2	0.927	-6.471	Very Good	Not good correlation	0.0084	0.0018
Eq-8	$y_s = k_s * \left(\frac{b}{y}\right)^{C_1} * y$	0.92	0.671	0.2	0.900	-3.316	Very Good	Not good correlation	0.0072	0.0019
Eq-9	$y_s = k_s * \left(\frac{b}{y}\right)^{C_1} * d_{50} * \left(\frac{V}{V_c}\right)^{C_2}$	159.91	0.526	0.2	0.5677	0.2780	Satisfactory	Unsatisfactory	0.02	0.016
Eq-10	$y_s = k_s * \left(\frac{b}{y}\right)^{C_1} * d_{50} * \left(\frac{V_c}{V}\right)^{C_2}$	161.03	0.518	0.2	0.5629	0.2408	Satisfactory	Unsatisfactory	0.02	0.016

[1]Moriasi et al. (2007)

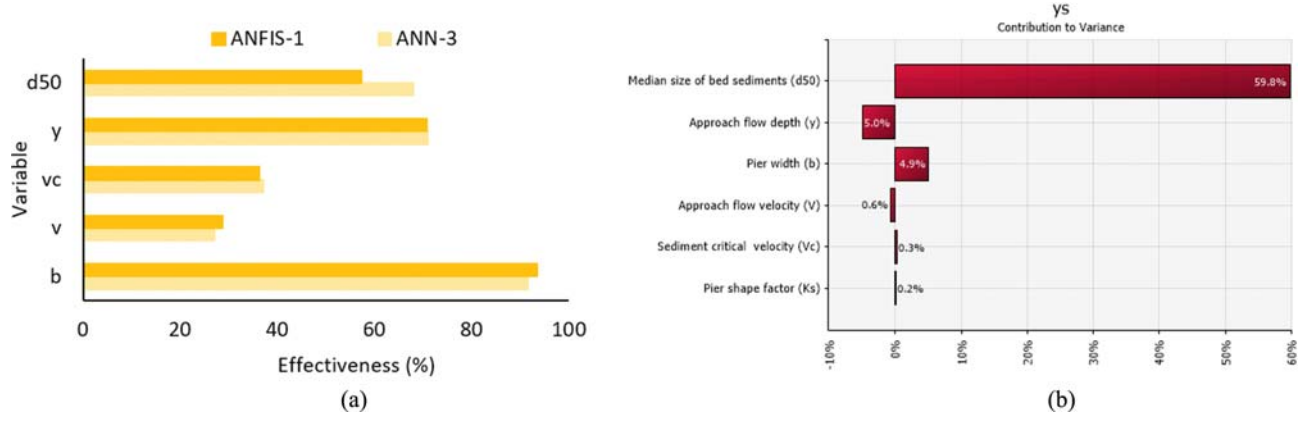

Fig. 12. Scenario Analysis and Sensitivity Analysis Results for Scour Depth Prediction, (a) Scenario Analysis for AI-Based Approaches, (b) Sensitivity Analysis Using DAEE

types of ANFIS models regarding performance. Five kinds of ANN training functions with various architectures showed excellent performance with overall NSE values of 0.82 to 0.986 (and MSE between 0.0000178 and 0.00064) with 10 neurons in hidden layers. The ANN-training function (BFGS Quasi-Newton BP) outperformed all the other functions; however, the Levenberg-Marquardt Backpropagation and Bayesian Regularization training functions also produced 'very good' results with 2nd and 3rd merit places. Concerning the architecture of ANN models, the DL model with 10 neurons in hidden layers is the top-level model compared to the 5 or 15-neuron architecture. Various combinations of input variables used in ANN revealed that the combination with four or five input variables performs better than the other with fewer input parameters. GRG optimization can identify parameters for estimating local scour around a bridge pier using empirical equations, which remained daunting. The declining performance of the validation process compared to calibration revealed that it is difficult to establish an empirical equation for estimating local scour around a bridge pier, which may work over an extensive range of data sets. The sensitivity analysis shows that the pier dimensions facing the flow (the pier width or its diameter) are the most influencing parameter in the estimation

of local scour. Future studies should investigate the impact of different pier shapes on scouring to overcome the limitations of the present study. Investigating the impact of various shapes of bridge piers and sustainable hooked collar countermeasures to reduce scour around a single bridge pier and a group of bridge piers may be a potential future research topic.

Acknowledgments

Authors also thank "The US Department of the Interior," *US Geol. Surv. Reston, VA, USA"* for providing access to scour data. The Researchers would like to thank the Deanship of Graduate Studies and Scientific Research at Qassim University for financial support (QU-APC-2024-9/1).

ORCID

Abdul Razzaq Ghumman https://orcid.org/0000-0002-4439-2013
Husnain Haider https://orcid.org/0000-0002-8600-8315
Ibrahim Saleh Al Salamah https://orcid.org/0000-0001-7880-8964
Md. Shafiquzzaman https://orcid.org/0000-0003-0226-9823
Abdullah Alodah https://orcid.org/0000-0002-0815-4579
Mohammad Alresheedi https://orcid.org/0000-0002-7322-3235
Rashid Farooq https://orcid.org/0000-0002-4763-7645
Afzal Ahmed https://orcid.org/0000-0002-8555-7013
Ghufran Ahmed Pasha https://orcid.org/0000-0002-7557-5373

References

Abadie J (1969) Generalization of the Wolfe reduced gradient method to the case of non-linear constraints. *Optimization*, 37-47

Abd El-Hady Rady R (2020) Prediction of local scour around bridge piers: Artificial-intelligence-based modeling versus conventional regression methods. *Applied Water Science* 10(2):57, DOI: 10.1007/s13201-020-1140-4

Afzali SH (2016) New model for determining local scour depth around piers. *Arabian Journal of Science and Engineering* 41(10):3807-3815, DOI: 10.1007/s13369-015-1983-4

Akhlaghi E, Babarsad MS, Derikvand EM, Abedini M (2020) Assessment the effects of different parameters to rate scour around single piers and pile groups: A review. *Archives of Computational Methods in Engineering* 27(1):183-197, DOI: 10.1007/s11831-018-09304-w

Alharbi S, Mills G (2022) Assessment of exposure to flash flooding in an arid environment: A case study of the jeddah city neighborhood abruq ar rughamah, saudi arabia. In: Wadi Flash Floods: Challenges and Advanced Approaches for Disaster Risk Reduction. Springer Nature Singapore, 383-397

Annad M, Lefkir A (2022) Analytic network process for local scour formula ranking with parametric sensitivity analysis and soil class clustering. *Water Supply* 22(11):8287-8304, DOI: 10.2166/ws.2022.357

Annad M, Lefkir A, Mammar-kouadri M, Bettahar I (2021) Development of a local scour prediction model clustered by soil class. *Water Practice & Technology* 16(4):1159-1172, DOI: 10.2166/wpt.2021.065

Arifin F, Robbani H, Annisa T, Ma'Arof N (2019) Variations in the number of layers and the number of neurons in artificial neural networks: Case study of pattern recognition. *Journal of Physics: Conference Series* 1413(1):12016, DOI: 10.1088/1742-6596/1413/1/012016

Arneson LA, Zevenbergen LW, Lagasse PF, Clopper PE (2012) Evaluating scour at bridges. Report No. FHWA-HIF-12-003 HEC-18, National Highway Institute, Arlington, VA, USA

Azamathulla HM, Ghani AA, Zakaria NA, Guven A (2010) Genetic programming to predict bridge pier scour. *Journal of Hydraulic Engineering* 136(3):165, DOI: 10.1061/(ASCE)HY.1943-7900.0000133

Benedict ST, Caldwell AW (2014) A pier-scour database: 2427 Field and Laboratory Measurements of Pier Scour, Data Series No. 845, US Department of the Interior, US Geol. Surv. Reston, VA, USA

Briaud JL, Ting FCK, Chen HC, Gudavalli R, Perugu S, Wei G (1999) SRICOS: Prediction of scour rate in cohesive soils at bridge piers. *Journal of Geotechnical and Geoenvironmental Engineering* 125(4):237-246, DOI: 10.1061/(ASCE)1090-0241(1999)125:4(237)

Cao J, Chen J, Zhu D, Wei S (2021) Evaluation of local scour calculation equations for bridge piers in sandy riverbed. *IOP Conference Series: Earth and Environmental Science* 692(4):042022, DOI: 10.1088/1755-1315/692/4/042022

Chabert J (1956) Etude des affouillements autour des piles de ponts. Laboratoire National d'Hydraulique, Chatou

Chavan R, Gualtieri P, Kumar B (2019) Turbulent flow structures and scour hole characteristics around circular bridge piers over non-uniform sand bed channels with downward seepage. *Water* 11(8):1580, DOI: 10.3390/w11081580

Chavan R, Kumar B (2020) Downward seepage effects on dynamics of scour depth and migrating dune-like bedforms at tandem piers. *Canadian Journal of Civil Engineering* 47(1):13-24, DOI: 10.1139/cjce-2017-0640

Choi SU, Choi S (2022) Prediction of local scour around bridge piers in the cohesive bed using support vector machines. *KSCE Journal of Civil Engineering* 26(5):2174-2182, DOI: 10.1007/s12205-022-1803-9

Ciancimino A, Anastasopoulos I, Foti S, Gajo A (2022) Numerical modelling of the effects of foundation scour on the response of a bridge pier. *Acta Geotech* 17(9):3697-3717, DOI: 10.1007/s11440-022-01591-9

Cikojević A, Gilja G, Kuspilić N (2019) Sensitivity analysis of empirical equations applicable on bridge piers in sand-bed rivers, Proceedings of the 16th International Symposium on Water Management and Hydraulic Engineering, September 5-7, Skopje, Republic of Macedonia

Dang NM, Tran Anh D, Dang TD (2021) ANN optimized by PSO and Firefly algorithms for predicting scour depths around bridge piers, *Engineering with Computers* 37(1):293-303, DOI: 10.1007/s00366-019-00824-y

Dimitriadis P, Koutsoyiannis D, Iliopoulou T, Papanicolaou P (2021) A global-scale investigation of stochastic similarities in marginal distribution and dependence structure of key hydrological-cycle processes. *Hydrology* 8(2):59, DOI: 10.3390/hydrology8020059

Ettema R (1980) Scour at bridge piers: A report submitted to the National Roads Board. PhD Thesis, The University of Auckland, Auckland, New Zealand

Farooq R, Ghumman AR, Ahmed A, Latif A, Masood A (2021) Performance evaluation of scour protection around a bridge pier through experimental approach. *Tehnički Vjesnik* 28(6):1975-1982, DOI: 10.17559/TV-20200213211932

Fattah MY, Hassan WH, Rasheed SE (2018) Behavior of flexible buried pipes under geocell reinforced subbase subjected to repeated loading. *International Journal of Geotechnical Earthquake Engineering* 9(1):22-41, DOI: 10.4018/IJGEE.2018010102

FHWA (1998) Recording and coding guide for the structural inventory and appraisal of the nations' bridges. Report No. FHWA-PD-96-001, US Department of Transportation, Federal Highway Administration. Office of Engineering, Washigton DC, USA

Fouli H, Elsebaie IH (2016) Reducing local scour at bridge piers using an upstream subsidiary triangular pillar. *Arabian Journal of Geosciences* 9(12):598, DOI: 10.1007/s12517-016-2615-3

Hafez YI (2016) Mathematical modeling of local scour at slender and wide bridge piers. *Journal of Fluids* 2016:1-19, DOI: 10.1155/2016/4835253

Hamidifar H, Zanganeh-Inaloo F, Carnacina I (2021) Hybrid scour depth prediction equations for reliable design of bridge piers. *Water* 13(15):2019, DOI: 10.3390/w13152019

Hassan WH, Hussein HH, Alshammari MH, Jalal HK, Rasheed SE (2022) Evaluation of gene expression programming and artificial neural networks in PyTorch for the prediction of local scour depth around a bridge pier. *Results in Engineering* 13:100353, DOI: 10.1016/j.rineng.2022.100353

Hassan WH, Jalal HK (2021) Prediction of the depth of local scouring at a bridge pier using a gene expression programming method. *SN Applied Sciences* 3(2):159, DOI: 10.1007/s42452-020-04124-9

Huang J, Yu H, Guan X, Wang G, Guo R (2016) Accelerated dryland expansion under climate change. *Nature Climate Change* 6(2):166-171, DOI: 10.1038/nclimate2837

Imhof D (2004) Risk assessment of existing bridge structures. PhD Thesis, University of Cambridge, Cambridge, UK

Jalal HK, Hassan WH (2020) Three-dimensional numerical simulation of local scour around circular bridge pier using Flow-3D software. *IOP Conference Series: Materials Science and Engineering* 745(1): 12150, DOI: 10.1088/1757-899X/745/1/012150

Khassaf SI, Ahmed SI (2021) Development an empirical formula to calculate the scour depth at different shapes of non-uniform piers. *Journal of Physics: Conference Series* 1973(1):012179, DOI: 10.1088/1742-6596/1973/1/012179

Lasdon LS, Waren AD, Jain A, Ratner M (1978) Design and testing of a generalized reduced gradient code for non-linear programming. *ACM Transactions on Mathematical Software* 4(1):34-50, DOI: 10.1145/355769.355773

Liang F, Wang C, Yu X (2019) Performance of existing methods for estimation and mitigation of local scour around bridges: Case studies. *Journal of Performance of Constructed Facilities* 33(6):4019060, DOI: 10.1061/(ASCE)CF.1943-5509.0001329

Lin C, Han J, Bennett C, Parsons RL (2014) Case history analysis of bridge failures due to scour. *Climatic Effects on Pavement and Geotechnical Infrastructure* 2014:204-216, DOI: 10.1061/9780784413326.021

Maddison B (2012) Scour failure of bridges. *Proceedings of the Institution of Civil Engineers-forensic Engineering* 165(1):39-52, DOI: 10.1680/feng.2012.165.1.39

Melville BW (1984) Live-bed scour at bridge piers. *Journal of Hydraulic Engineering* 110(9):1234-1247, DOI: 10.1061/(ASCE)0733-9429(1984)110:9(1234)

Mohammadpour R (2017) Prediction of local scour around complex piers using GEP and M5-Tree. *Arabian Journal of Geosciences* 10(18):416, DOI: 10.1007/s12517-017-3203-x

Mohammadpour R, Ghani AA, Sabzevari T, Fared Murshed M (2021) Local scour around complex abutments. *ISH Journal of Hydraulic Engineering* 27(1):165-173, DOI: 10.1080/09715010.2019.1607783

Moriasi DN, Arnold JG, Van Liew MW, Bingner RL, Harmel RD, Veith TL (2007) Model evaluation guidelines for systematic quantification of accuracy in watershed simulations. *Transactions of ASABE* 50(3): 885-900, DOI: 10.13031/2013.23153

Moussa YAM (2013) Modeling of local scour depth downstream hydraulic structures in trapezoidal channel using GEP and ANNs. *Ain Shams Engineering Journal* 4(4):717-722, DOI: 10.1016/j.asej.2013.04.005

Muzzammil M, Alama J, Danish M (2015) Scour prediction at bridge piers in cohesive bed using gene expression programming. *Aquatic Procedia* 4:789-796, DOI: 10.1016/j.aqpro.2015.02.098

Namaee MR, Li Y, Sui J, Whitcombe T (2018) Comparison of three commonly used equations for calculating local scour depth around bridge pier under ice covered flow condition. *World Journal of Engineering and Technology* 6(2):50-62

Ogunbo JN, Alagbe OA, Oladapo MI, Shin C (2020) N-hidden layer artificial neural network architecture computer code: Geophysical application example. *Heliyon* 6(6):e04108, DOI: 10.1016/j.heliyon.2020.e04108

Oğuz K, Bor A (2022) Prediction of local scour around bridge piers using hierarchical clustering and adaptive genetic programming. *Applied Artificial Intelligence* 36(1), DOI: 10.1080/08839514.2021.2001734

Omara H, Abdeelaal GM, Nadaoka K, Tawfik A (2020) Developing empirical formulas for assessing the scour of vertical and inclined piers. *Marine Georesources and Geotechnology* 38(2):133-143, DOI: 10.1080/1064119X.2018.1559901

Onen F (2014) Prediction of Scour at a Side-Weir with GEP, ANN and Regression Models. *Arabian Journal of Science and Engineering* 39(8):6031-6041, DOI: 10.1007/s13369-014-1244-y

Pal M, Singh NK, Tiwari NK (2011) Support vector regression based modeling of pier scour using field data. *Engineering Applications of Artificial Intelligence* 24(5):911-916, DOI: 10.1016/j.engappai.2010.11.002

Pandey M, Zakwan M, Khan MA, Bhave S (2020) Development of scour around a circular pier and its modelling using genetic algorithm. *Water Supply* 20(8):3358-3367, DOI: 10.2166/ws.2020.244

Park CW, Park HI, Cho YK (2017) Evaluation of the applicability of pier local scour formulae using laboratory and field data. *Marine Georesources Geotechnology* 35(1):1-7, DOI: 10.1080/1064119X.2014.954658

Parola AC, Hagerty DJ, Mueller DS, Melville BW, Parker G, Usher JS (1997) The need for research on scour at bridge crossings, 1997. Proceedings of the 27th IAHR World Congress. San Fransisco, CA, USA

Pizarro A, Manfreda S, Tubaldi E (2020) The science behind scour at bridge foundations: A review. *Water* 12(2):374, DOI: 10.3390/w12020374

Pizarro A, Samela C, Fiorentino M, Link O, Manfreda S (2017) BRISENT: An entropy-based model for bridge-pier scour estimation under complex hydraulic scenarios. *Water* 9(11):889, DOI: 10.3390/w9110889

Pregnolato M, Winter AO, Mascarenas D, Sen AD, Bates P, Motley MR (2022) Assessing flooding impact to riverine bridges: An integrated analysis. *Natural Hazards and Earth System Sciences* 22(5):1559-1576, DOI: 10.5194/nhess-22-1559-2022

Saad NY, Fattouh EM, Mokhtar M (2021) Effect of L-shaped slots on scour around a bridge abutment. *Water Practice and Technology* 16(3):935-945, DOI: 10.2166/wpt.2021.037

Sarshari E, Mullhaupt P (2015) Application of artificial neural networks in assessing the equilibrium depth of local scour around bridge piers. ASME 2015 34th International Conference on Ocean, Offshore and Arctic Engineering, May 31–June 5, St. John's, NL, Canada

Sharafati A, Tafarojnoruz A, Yaseen ZM (2020) New stochastic modeling strategy on the prediction enhancement of pier scour depth in cohesive

bed materials. *Journal of Hydroinformatics* 22(3):457-472, DOI: 10.2166/hydro.2020.047

Sheela KG, Deepa SN (2013) Review on methods to fix number of hidden neurons in neural networks. *Mathematical Problems in Engineering* 2013:425740, DOI: 10.1155/2013/425740

Sreedhara BM, Patil AP, Pushparaj J, Kuntoji G, Naganna SR (2021) Application of gradient tree boosting regressor for the prediction of scour depth around bridge piers. *Journal of Hydroinformatics* 23(4): 849-863, DOI: 10.2166/hydro.2021.011

Wang C, Yu X, Liang F (2017) Comparison and estimation of the local scour depth around pile groups and wide piers. In Geotechnical Frontiers, American Scciety ofCivil Engineers, Reston, VA, USA, 11-19

Wardhana K, Hadipriono FC (2003) Analysis of recent bridge failures in the United States. *Journal of Performance of Constricted Facilities* 17(3):144-150, DOI: 10.1061/(ASCE)0887-3828(2003)17:3(144)

Youssef AM, Abu-Abdullah MM, AlFadail EA, Skilodimou HD, Bathrellos GD (2018) The devastating flood in the arid region a consequence of rainfall and dam failure: Case study. *Al-Lith flood on 23th November 2018, Kingdom of Saudi Arabia, Zeitschrift für Geomorphol* 63(1):115-136, DOI: 10.1127/zfg/2021/0672

Zhang B, Zhao H, Tan C, OBrien EJ, Fitzgerald PC, Kim CW (2022) Laboratory investigation on detecting bridge scour using the indirect measurement from a passing vehicle. *Remote Sensing* 14(13):3106, DOI: 10.3390/rs14133106